读书报告

呼吸治疗师:王鹏

2015－4－30

华西医院重症医学科

AJRCCM 摘要阅读

Calcium Channel Blocker Reduces Airway Remodeling in Severe Asthma. A Proof-of-Concept Study

Rationale: Severe asthma is a major public health issue throughout the world. Increased bronchial smooth muscle (BSM) mass, a characteristic feature of airway remodeling in severe asthma, is associated with resistance to high-intensity treatment and poor prognosis. *In vitro*, the Ca^{2+}-channel blocker gallopamil decreased the proliferation of BSM cells from patients with severe asthma.

Objectives: We conducted a double-blind, randomized, placebo-controlled study to evaluate the effect of gallopamil on airway remodeling in patients with severe asthma.

Methods: Subjects received either gallopamil (n = 16) or placebo (n = 15) for 1 year and were monitored for an additional 3-month period. Airway remodeling was analyzed at baseline and after treatment phase using both fiberoptic bronchoscopy and computed tomography scan. The primary end point was the BSM area. Secondary end points included normalized BSM thickness and frequency of asthma exacerbations.

Measurements and Main Results: BSM area was reduced in the gallopamil group (baseline vs. end of treatment) but was unchanged in the placebo group. Between-group differences in BSM area were not significantly different in gallopamil versus placebo groups. By contrast, between-group differences in normalized BSM thickness were significantly different between the two groups. The mean number of exacerbations per month was not different during the treatment phase in gallopamil versus placebo group but was significantly lower in patients previously treated with gallopamil during the follow-up period. There were no differences between the groups with respect to overall side effects.

Conclusions: Gallopamil treatment for 12 months reduces BSM remodeling and prevents the occurrence of asthma exacerbations

Human Trachealis and Main Bronchi Smooth Muscle Are Normo-responsive in Asthma

Measurements and Main Results: Main bronchi and tracheal ASM were significantly hyposensitive in subjects with asthma compared with control subjects. Trachea and main bronchi did not show significant differences in reactivity to methacholine and unloaded tissue shortening velocity (Vmax) compared with control subjects. There were no significant differences in responses to deep inspiration, with or without superimposed tidal breathing oscillations. No significant correlations were found between age, body mass index, or sex and sensitivity, reactivity, or Vmax.

Conclusions: Our data show that, in contrast to some animal models of AHR, human tracheal and main bronchial smooth muscle contractility is not increased in asthma.

Hypoxic Epithelial Necrosis Triggers Neutrophilic Inflammation via IL-1 Receptor Signaling in Cystic Fibrosis Lung Disease

Rationale: In many organs, hypoxic cell death triggers sterile neutrophilic inflammation via IL-1R signaling. Although hypoxia is common in airways from patients with cystic fibrosis (CF), its role in neutrophilic inflammation remains unknown. We recently demonstrated that hypoxic epithelial necrosis caused by airway mucus obstruction precedes neutrophilic inflammation in *Scnn1b*-transgenic (*Scnn1b*-Tg) mice with CF-like lung disease.

Objectives: To determine the role of epithelial necrosis and IL-1R signaling in the development of neutrophilic airway inflammation, mucus obstruction, and structural lung damage in CF lung disease.

Methods: We used genetic deletion and pharmacologic inhibition of IL-1R in *Scnn1b*-Tg mice and determined effects on airway epithelial necrosis; levels of IL-1α, keratinocyte chemoattractant, and neutrophils in bronchoalveolar lavage; and mortality, mucus obstruction, and structural lung damage. Furthermore此外, we analyzed lung tissues from 21 patients with CF and chronic obstructive pulmonary disease and 19 control subjects for the presence of epithelial necrosis.

Measurements and Main Results: Lack of IL-1R had no effect on epithelial necrosis and elevated IL-1α, but abrogated airway neutrophilia and reduced mortality, mucus obstruction, and emphysema in *Scnn1b*-Tg mice. Treatment of adult *Scnn1b*-Tg mice with the IL-1R antagonist anakinra had protective effects on neutrophilic inflammation and emphysema. Numbers of necrotic airway epithelial cells were elevated and correlated with mucus obstruction in patients with CF and chronic obstructive pulmonary disease.

Conclusions: Our results support an important role of hypoxic epithelial necrosis in the pathogenesis of neutrophilic inflammation independent of bacterial infection and suggest IL-1R as a novel target for antiinflammatory therapy in CF and potentially other mucoobstructive airway diseases.

Regulatory T-Cell Impairment in Cystic Fibrosis Patients with Chronic *Pseudomonas* Infection

Rationale: Patients with cystic fibrosis (CF) lung disease have chronic airway inflammation driven by disrupted balance of T-cell (Th17 and Th2) responses. Regulatory T cells (Tregs) dampen T-cell activation, but their role in CF is incompletely understood.

Objectives: To characterize numbers, function, and clinical impact of Tregs in CF lung disease.

Methods: Tregs were quantified in peripheral blood and airway samples from patients with CF and from lung disease control patients without CF and healthy control subjects. The role of *Pseudomonas aeruginosa* and CF transmembrane conductance regulator (CFTR) in Treg regulation was analyzed by using *in vitro* and murine *in vivo* models.

Measurements and Main Results: Tregs were decreased in peripheral blood and airways of patients with CF compared with healthy controls or lung disease patients without CF and correlated positively with lung function parameters. Patients with CF with chronic *P. aeruginosa* infection had lower Tregs compared with patients with CF without *P. aeruginosa* infection. Genetic knockout, pharmacological inhibition, and *P. aeruginosa* infection studies showed that both *P. aeruginosa* and CFTR contributed to Treg dysregulation in CF. Functionally, Tregs from patients with CF or from $Cftr^{-/-}$ mice were impaired in suppressing conventional T cells, an effect that was enhanced by *P. aeruginosa* infection. The loss of Tregs in CF affected memory, but not naive Tregs, and manifested gradually with disease progression.

Conclusions: Patients with CF who have chronic *P. aeruginosa* infection show an age-dependent, quantitative, and qualitative impairment of Tregs. Modulation of Tregs represents a novel strategy to rebalance T-cell responses, dampen inflammation, and ultimately improve outcomes for patients with infective CF lung disease.

Improving Selection Criteria for Lung Cancer Screening. The Potential Role of Emphysema

Rationale: Lung cancer (LC) screening using low-dose chest computed tomography is now recommended in several guidelines using the National Lung Screening Trial (NLST) entry criteria (age, 55–74; ≥30 pack-years; tobacco cessation within the previous 15 yr for former smokers). Concerns exist about their lack of sensitivity.

Objectives: To evaluate the performance of NLST criteria in two different LC screening studies from Europe and the United States, and to explore the effect of using emphysema as a complementary criterion.

Methods: Participants from the Pamplona International Early Lung Action Detection Program (P-IELCAP; n = 3,061) and the Pittsburgh Lung Screening Study (PLuSS; n = 3,638) were considered. LC cumulative frequencies, incidence densities, and annual detection rates were calculated in three hypothetical cohorts, including subjects who met NLST criteria alone, those with computed tomography–detected emphysema, and those who met NLST criteria and/or had emphysema.

Measurements and Main Results: Thirty-six percent 36% and 59% of P-IELCAP and PLuSS participants, respectively, met NLST criteria. Among these, higher LC incidence densities and detection rates were observed. However, applying NLST criteria to our original cohorts would miss as many as 39% of all LC. Annual screening of subjects meeting either NLST criteria or having emphysema detected most cancers (88% and 95% of incident LC of P-IELCAP and PLuSS, respectively) despite reducing the number of screened participants by as much as 52%.

Conclusions: LC screening based solely on NLST criteria could miss a significant number of LC cases. Combining NLST criteria and emphysema to select screening candidates results in higher LC detection rates and a lower number of cancers missed.

Topographic Diversity of the Respiratory Tract Mycobiome and Alteration in HIV and Lung Disease

Rationale: Microbiome studies typically focus on bacteria, but fungal species are common in many body sites and can have profound effects on the host. Wide gaps exist in the understanding of the fungal microbiome (mycobiome) and its relationship to lung disease.

Objectives: To characterize the mycobiome at different respiratory tract levels in persons with and without HIV infection and in HIV-infected individuals with chronic obstructive pulmonary disease (COPD).

Methods: Oral washes (OW), induced sputa (IS), and bronchoalveolar lavages (BAL) were collected from 56 participants. We performed 18S and internal transcribed spacer sequencing and used the neutral model to identify fungal species that are likely residents of the lung. We used ubiquity–ubiquity plots, random forest, logistic regression, and metastats to compare fungal communities by HIV status and presence of COPD.

Measurements and Main Results: Mycobiomes of OW, IS, and BAL shared common organisms, but each also had distinct members. *Candida* was dominant in OW and IS, but BAL had 39 fungal species that were disproportionately more abundant than in the OW. Fungal communities in BAL differed significantly by HIV status and by COPD, with *Pneumocystis jirovecii*（PCP）significantly overrepresented in both groups. Other fungal species were also identified as differing in HIV and COPD.

Conclusions: This study systematically examined the respiratory tract mycobiome in a relatively large group. By identifying *Pneumocystis* and other fungal species as overrepresented in the lung in HIV and in COPD, it is the first to determine alterations in fungal communities associated with lung dysfunction and/or HIV, highlighting the clinical relevance of these findings.

Bactericidal Activity of Pyrazinamide and Clofazimine Alone and in Combinations with Pretomanid and Bedaquiline

Rationale: New regimens shorten tuberculosis treatment and manage patients with drug-resistant tuberculosis who are infected with HIV are urgently needed. Experimental and clinical evidence suggests that the new drugs bedaquiline (B) and pretomanid (Pa), combined with an existing drug, pyrazinamide (Z), and a repurposed drug, clofazimine (C), may assist treatment shortening of drug-susceptible and drug-resistant tuberculosis.

Objectives: To evaluate the 14-day bactericidal activity of C and Z in monotherapy and in combinations with Pa and B.

Methods: Groups of 15 treatment-naïve, sputum smear–positive patients with pulmonary tuberculosis were randomized to receive combinations of B with Z-C, Pa-Z, Pa-Z-C, and Pa-C, or C or Z alone, or standard combination treatment for 14 days. The primary endpoint was the mean daily fall in $\log_{10}$ *Mycobacterium tuberculosis* CFU per milliliter毫升 sputum estimated by joint nonlinear mixed-effects Bayesian regression modeling.

Measurements and Main Results: Estimated activities were 0.167 (95% confidence interval [CI], 0.075–0.257) for B-Pa-Z, 0.151 (95% CI, 0.071–0.232) for standard treatment, 0.124 (95% CI, 0.035–0.214) for B-Z-C, 0.115 (95% CI, 0.039–0.189) for B-Pa-Z-C, and 0.076 (95% CI, 0.005–0.145) for B-Pa-C. Z alone had modest 最低的activity (0.036; 95% CI, −0.026 to 0.099). C had no activity alone (−0.017; 95% CI, −0.085 to 0.053) or in combinations. Treatments were well tolerated and safe.

Conclusions: B-Pa-Z, including two novel agents without resistance in prevalent *M. tuberculosis* strains, is a potential new tuberculosis treatment regimen. C had no measurable activity in the first 14 days of treatment.

Sleep in the Intensive Care Unit

Sleep is an important physiologic process, and lack of sleep is associated with a host of adverse outcomes. Basic and clinical research has documented the important role circadian rhythm plays in biologic function. Critical illness is a time of extreme vulnerability for patients, and the important role sleep may play in recovery for intensive care unit (ICU) patients is just beginning to be explored. This concise clinical review focuses on the current state of research examining sleep in critical illness. We discuss sleep and circadian rhythm abnormalities that occur in ICU patients and the challenges to measuring alterations in circadian rhythm in critical illness and review methods to measure sleep in the ICU, including polysomnography, actigraphy, and questionnaires. We discuss data on the impact of potentially modifiable disruptors to patient sleep, such as noise, light, and patient care activities, and report on potential methods to improve sleep in the setting of critical illness. Finally, we review the latest literature on sleep disturbances that persist or develop after critical illness.

Cardiotoxicity during Invasive Pneumococcal Disease

Streptococcus pneumoniae is the leading cause of community-acquired pneumonia and sepsis, with adult hospitalization linked to approximately 19% incidence of an adverse cardiac event (e.g., heart failure, arrhythmia, infarction). Herein, we review the specific host–pathogen interactions that contribute to cardiac dysfunction during invasive pneumococcal disease: (*1*) cell wall–mediated inhibition of cardiomyocyte contractility; (*2*) the new observation that *S. pneumoniae* is capable of translocation into the myocardium and within the heart, forming discrete, nonpurulent, microscopic lesions that are filled with pneumococci; and (*3*) the bacterial virulence determinants, pneumolysin and hydrogen peroxide, that are most likely responsible for cardiomyocyte cell death. Pneumococcal invasion of heart tissue is dependent on the bacterial adhesin choline-binding protein A that binds to laminin receptor on vascular endothelial cells and binding of phosphorylcholine residues on pneumococcal cell wall to platelet-activating factor receptor. These are the same interactions responsible for pneumococcal translocation across the blood–brain barrier during the development of meningitis. We discuss these interactions and how their neutralization, either with antibody or therapeutic agents that modulate platelet-activating factor receptor expression, may confer protection against cardiac damage and meningitis. Considerable collagen deposition was observed in hearts of mice that had recovered from invasive pneumococcal disease. We discuss the possibility that cardiac scar formation after severe pneumococcal infection may explain why individuals who are hospitalized for pneumonia are at greater risk for sudden death up to 1 year after infection.

Asthma–COPD Overlap. Clinical Relevance of Genomic Signatures of Type 2 Inflammation in Chronic Obstructive Pulmonary Disease

Measurements and Main Results: The 200 genes most differentially expressed in asthma versus healthy control subjects were enriched among genes associated with more severe airflow obstruction in these COPD cohorts ($P < 0.001$), suggesting significant gene expression overlap. A higher T2S score was associated with decreased lung function ($P < 0.001$), but not asthma history, in both COPD cohorts. Higher T2S scores correlated with increased airway wall eosinophil counts ($P = 0.003$), blood eosinophil percentage ($P = 0.03$), bronchodilator reversibility ($P = 0.01$), and improvement in hyperinflation after corticosteroid treatment ($P = 0.019$) in GLUCOLD.

Conclusions: These data identify airway gene expression alterations that can co-occur in asthma and COPD. The association of the T2S score with increased severity and “asthma-like” features (including a favorable corticosteroid response) in COPD suggests that Th2 inflammation is important in a COPD subset that cannot be identified by clinical history of asthma.

Computed Tomography Predictors of Response to Endobronchial Valve Lung Reduction Treatment. Comparison with Chartis

Measurements and Main Results: FI ($P < 0.0001$) and low attenuation clusters($P = 0.01$) measured in the treated lobe and vascular volumetric percentage of patient's detected smallest vessels ($P = 0.02$) were identified as the primary QCT predictors of LVR outcome. Accuracy for QCT patient selection based on these primary predictors was comparable to Chartis (78.8 vs. 75.8%).

Conclusions: Quantitative CT led to comparable results to Chartis for classifying LVR and is a promising tool to effectively select patients for valve-based LVR procedures.

Randomized Trial of Endobronchial Ultrasound–guided Transbronchial Needle Aspiration (EBUS-TBNA) under General Anesthesia versus Moderate Sedation

Measurements and Main Results: The main outcome was “diagnostic yield,” defined as the percentage of patients for whom EBUS-TBNA rendered a specific diagnosis. One hundred and forty-nine patients149人 underwent EBUS-TBNA, 75 under GA and 74 under MS. Demographic and baseline clinical characteristics were well balanced. Two hundred and thirty-six lymph nodes (LNs) and six masses were sampled in the GA group (average, 3.2 ± 1.9 sites/patient), and 200 LNs and six masses in the MS group (average, 2.8 ± 1.5 sites/patient) ($P = 0.199$). The diagnostic yield was 70.7% (53 of 75) and 68.9% (51 of 74) for the GA group and MS group, respectively ($P = 0.816$). The sensitivity was 98.2% in the GA group (confidence interval, 97–100%) and 98.1% in the MS group (confidence interval, 97–100%) ($P = 0.979$). EBUS was completed in all patients in the GA group, and in 69 patients (93.3%) in the MS group ($P = 0.028$). There were no major complications or escalation of care in either group. Minor complications were more common in the MS group (29.6 vs. 5.3%) ($P < 0.001$). Most patients stated they “definitely would” undergo this procedure again in both groups ($P = 0.355$).

Conclusions: EBUS-TBNA performed under MS results in comparable diagnostic yield, rate of major complications, and patient tolerance as under GA. Future prospective multicenter studies are required to corroborate our findings.

Platelet Activation and Aggregation Promote Lung Inflammation and Influenza Virus Pathogenesis

Measurements and Main Results: Lungs of infected mice were massively infiltrated by aggregates of activated platelets. Platelet activation promoted influenza A virus pathogenesis. Activating protease-activated receptor 4, a platelet receptor for thrombin that is crucial for platelet activation, exacerbated influenza-induced acute lung injury and death. In contrast, deficiency in the major platelet receptor glycoprotein IIIa protected mice from death caused by influenza viruses, and treating the mice with a specific glycoprotein IIb/IIIa antagonist, eptifibatide, had the same effect. Interestingly, mice treated with other antiplatelet compounds (antagonists of protease-activated receptor 4, MRS 2179, and clopidogrel) were also protected from severe lung injury and lethal infections induced by several influenza strains.

Conclusions: The intricate relationship between hemostasis and inflammation has major consequences in influenza virus pathogenesis, and antiplatelet drugs might be explored to develop new antiinflammatory treatment against influenza virus infections.

Optimizing the Detection of Recent Tuberculosis Infection in Children in a High Tuberculosis–HIV Burden Setting

An Official American Thoracic Society/European Respiratory Society Statement: Research Questions in Chronic Obstructive Pulmonary Disease

Smoking-induced Skeletal Muscle Dysfunction. From Evidence to Mechanisms

Wogonin Induces Eosinophil Apoptosis and Attenuates Allergic Airway Inflammation

Measurements and Main Results: Wogonin induced time- and concentration-dependent human and mouse eosinophil apoptosis *in vitro*. Wogonin-induced eosinophil apoptosis occurred with activation of caspase-3 and was inhibited by pharmacological caspase inhibition. Wogonin administration attenuated allergic airway inflammation *in vivo* with reductions in BAL and interstitial eosinophil numbers, increased eosinophil apoptosis, reduced airway mucus production, and attenuated airway hyperresponsiveness. This wogonin-induced reduction in allergic airway inflammation was prevented by concurrent caspase inhibition *in vivo*.

Conclusions: Wogonin induces eosinophil apoptosis and attenuates allergic airway inflammation, suggesting that it has therapeutic potential for the treatment of allergic inflammation in humans.

Randomized Intubation with Polyurethane or Conical Cuffs to Prevent Pneumonia in Ventilated Patients

Measurements and Main Results: After excluding 17 patients who secondarily refused participation or had met an exclusion criterion, 604 were included in the intention-to-treat analysis. Cumulative tracheal colonization greater than 10^3cfu/ml at Day 2 was as follows (median [interquartile range]): cylindrical polyvinyl chloride, 0.66 (0.58–0.74); cylindrical polyurethane, 0.61 (0.53–0.70); conical polyvinyl chloride, 0.67 (0.60–0.76); and conical polyurethane, 0.62 (0.55–0.70) ($P = 0.55$). VAP developed in 77 patients (14.4%), and postextubational stridor developed in 28 patients (6.4%) ($P = 0.20$ and 0.28 between groups, respectively).

Conclusions: Among patients requiring mechanical ventilation, polyurethane and/or conically shaped cuffs were not superior to conventional cuffs in preventing tracheal colonization and VAP.

Rare Variants in *RTEL1* Are Associated with Familial Interstitial Pneumonia

Long-Term Exposure to Traffic Emissions and Fine Particulate Matter and Lung Function Decline in the Framingham Heart Study

Impaired Bone Morphogenetic Protein Receptor II Signaling in a Transforming Growth Factor-β–Dependent Mouse Model of Pulmonary Hypertension and in Systemic Sclerosis

Sex Affects Bone Morphogenetic Protein Type II Receptor Signaling in Pulmonary Artery Smooth Muscle Cells

Ampakines Enhance Weak Endogenous Respiratory Drive and Alleviat Apnea in Perinatal Rats

Genome-Wide Association Study of Short-Acting β_2-Agonists. A Novel Genome-Wide Significant Locus on Chromosome 2 near *ASB3*

House Dust Mites Induce Proliferation of Severe Asthmatic Smooth Muscle Cells via an Epithelium-Dependent Pathway

Rapid Automated Microscopy for Microbiological Surveillance of Ventilator-associated Pneumonia

Occupational Exposures Are Associated with Worse Morbidity in Patients with Chronic Obstructive Pulmonary Disease

Rationale: Links between occupational exposures and morbidity in individuals with established chronic obstructive pulmonary disease (COPD) remain unclear.

Objectives: To determine the impact of occupational exposures on COPD morbidity.

Methods: A job exposure matrix 模型(JEM) determined occupational exposure likelihood based on longest job in current/former smokers (n = 1,075) recruited as part of the Subpopulations and Intermediate Outcomes in COPD Study, of whom 721 had established COPD. Bivariate and multivariate linear regression models estimated the association of occupational exposure with COPD, and among those with established disease, the occupational exposure associations with 6-minute-walk distance (6MWD), the Modified Medical Research Council Dyspnea Scale (mMRC), the COPD Assessment Test (CAT), St. George's Respiratory Questionnaire (SGRQ), 12-item Short-Form Physical Component (SF-12), and COPD exacerbations requiring health care utilization, adjusting for demographics, current smoking status, and cumulative pack-years.

Measurements and Main Results: An intermediate/high risk of occupational exposure by JEM was found in 38% of participants. In multivariate analysis, those with job exposures had higher odds of COPD (odds ratio, 1.44; 95% confidence interval, 1.04–1.97). Among those with COPD, job exposures were associated with shorter 6MWDs (−26.0 m; $P = 0.006$); worse scores for mMRC (0.23; $P = 0.004$), CAT (1.8; $P = 0.003$), SGRQ (4.5; $P = 0.003$), and SF-12 Physical (−3.3; $P < 0.0001$); and greater odds of exacerbation requiring health care utilization (odds ratio, 1.55; $P = 0.03$).

Conclusions: Accounting for smoking, occupational exposure was associated with COPD risk and, for those with established disease, shorter walk distance, greater breathlessness, worse quality of life, and increased exacerbation risk. Clinicians should obtain occupational histories from patients with COPD because work-related exposures may influence disease burden.


往下看，
下面更精彩……

Heart–lung interactions during neurally adjusted ventilatory assist

David Berger1†, Stefan Bloechlinger1,2†, Jukka Takala1, Christer Sinderby3,4 and Lukas Brander1,5*

Introduction

- Cyclic increases in intrathoracic pressure during positive pressure ventilation may reduce venous return and increase the afterload of the right ventricle.

- Neurally adjusted ventilatory assist (NAVA) delivers inspiratory support in synchrony and in linear proportion to the neural inspiratory effort by using the electrical activity of the diaphragm (EAdi) to drive the ventilator .

- The inspiratory muscle activity, that is synchronous and proportional to assist delivery during NAVA, is likely to attenuate the increases in pleural pressure associated with conventional positive pressure ventilation.

- We therefore compared the short-term hemodynamic effects of three NAVA and three PSV levels using simultaneous analysis of intravascular, intracardiac, esophageal pressure (Pes), airway pressure, breathing pattern,and echocardiography in patients with impaired cardiac function, chronic obstructive pulmonary disease, or both.

Materials and methods

- The Ethics Committee of Canton Bern, Switzerland approved the protocol (KEK Nr 217–06). Recruitment lasted from March to November 2010. Written informed consent from the patient's family and deferred consent after recovery were obtained.

- The main inclusion criteria were invasive mechanical ventilation, pneumatic triggering, pulmonary artery catheter monitoring for clinical reasons, and at least one of the following: left ventricular ejection fraction ≤40%; inotropic drugs (dobutamine ≥2 μg/kg/minute or adrenaline ≥0.03 μg/kg/minute); pulmonary artery occlusion pressure ≥18 mmHg; or history of chronic obstructive pulmonary disease.

Study protocol

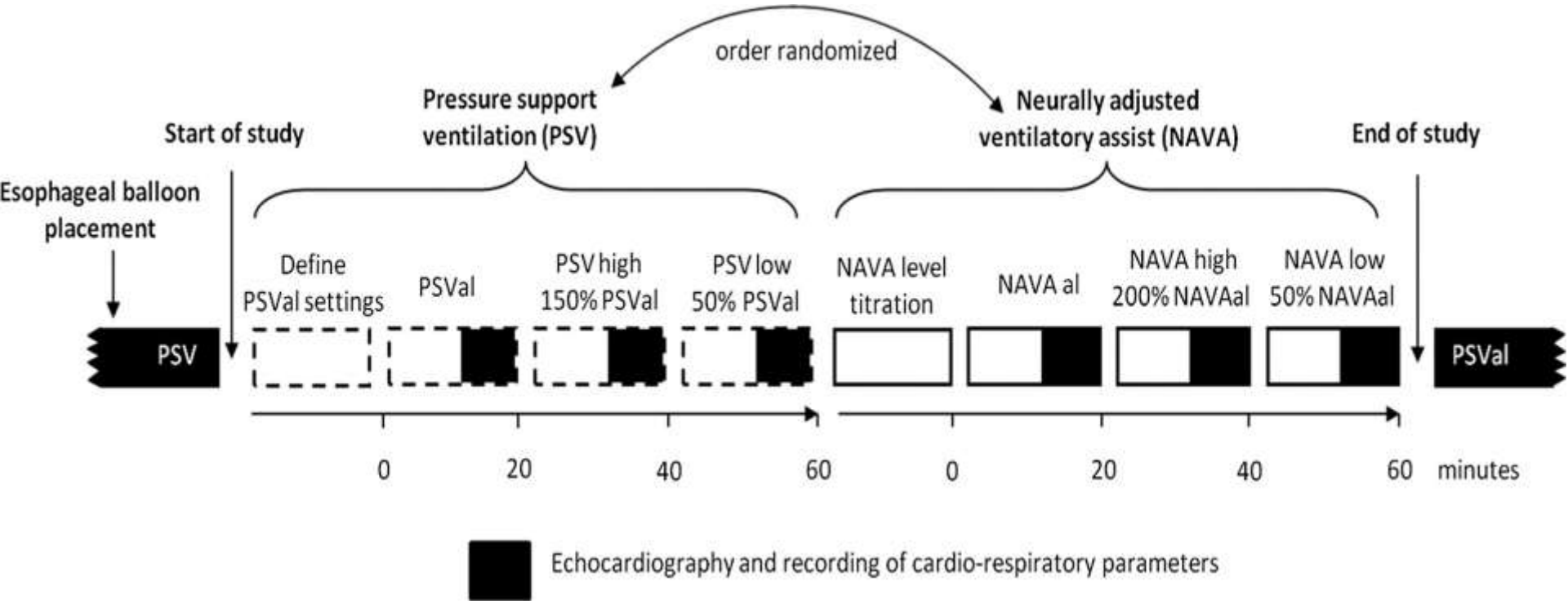

- Adequate PSV (PSVal) was set by an independent intensivist blinded for the EAdi and Pes aiming to achieve optimal patient comfort, avoid unassisted wasted inspiratory efforts, and minimize negative inspiratory deflections in central venous and pulmonary artery pressures (indicating inspiratory effort). PSVlow was 50% PSVal, and PSVhigh was 150% PSVal. Positive end-expiratory pressure (PEEP) and other prescribed ventilator settings were kept constant throughout the protocol.

- Adequate NAVA (NAVAal) was identified using a previously described titration procedure. NAVAlow was 50% NAVAal, and NAVAhigh was defined as the highest level sustaining a regular breathing pattern similar to that at NAVAal or 200% NAVAal, whichever occurred first.

- The order of the ventilatory modes was randomized. The six ventilator settings were applied for at least 20 minutes each. All medications including sedation (Richmond agitation and sedation scale of −1 to −2) remained unchanged.

Measurements

- Intravascular pressures, airway pressure, Pes, EAdi ,and airflow were recorded continuously(Neurovent Research Inc., Toronto, ON, Canada).Pulmonary artery occlusion pressure, right ventricular pressure, and blood gases were measured at the end of each experimental period.

- Two approaches were used to evaluate the hemodynamic responses. First, intravascular pressure and Pes during all breaths in each ventilator setting were averaged separately during inspiration and expiration. This was done in order to include the impact of variability in breathing pattern on hemodynamics. Transmural vascular pressures were obtained by subtraction of the time integral of Pes from the respective intravascular pressure. Changes of intravascular pressures from inspiration to expiration (cyclic pressure changes) were characterized by subtracting the mean expiratory pressure from the mean inspiratory pressure

- Second, representative single-breath cycles were manually selected for each experimental period. The selected breaths had mean inspiratory transpulmonary pressures equal to the mean of all breaths for the specific study period (the average breath). For each of these single breaths, the central venous pressure (CVP) was measured at the base of the c wave . The right ventricular isovolumetric pressure change was calculated as the difference between the base of the c wave of CVP and the pulmonary artery pressure (PAP) at valve opening , and the right ventricular total pressure generation was calculated as the pressure difference from the end-diastolic filling of the right ventricle (estimated as the base of the CVP c wave) to the systolic PAP.

- Pulsed wave Doppler profiles from both ventricular outflow tracts were recorded simultaneously with airway pressure during transthoracic echocardiography and were analyzed offline (Vivid 7, EchoPAC Dimension '06; GE Medical Systems, Glattbrugg, Switzerland). End-inspiratory and end-expiratory heart beats from three ventilatory cycles were analyzed for each condition. To characterize the effects of lung inflation on the Doppler flow profiles, the values at end inspiration were expressed as a percentage of the values at end expiration measured during the same breathing cycle. A value >100% would thus reflect a higher value during inspiration compared with expiration, and vice versa.

Statistical analysis

- Repeated-measures analysis of variance (within-subject factors: ventilation mode, support level) was used for analysis. Significant mode*support level interactions were analyzed post hoc within each mode between support levels using Sidak's correction (IBM SPSS 20.0.0; IBM Corp,Armonk, NY, USA). Data are presented as mean ± standard deviation. P <0.05 was considered significant.

Results

Table 1 Characteristics of individual patients

Patient number	PBW (kg)	BMI (kg/m^2)	SAPS II	ICU LOS (days)	Perioperative LVEF (%)	Prestudy PAOP (mmHg)	Prestudy cardiac index (l/minute/m^2)	Dobutamine during study (μg/kg/minute)	Cardiopulmonary diagnosis
1	72	26	42	1.8	35	15	1.4	3.1	CABG
2	60	24	34	0.9	31	14	2.6	3.8	CABG
3	57	30	37	1.0	40	12	3.2	0.0	CABG, COPD with cor pulmonale
4	50	31	35	0.9	35	8	1.6	3.4	CABG, aortic valve replacement
5	73	31	54	3.4	35	13	3.6	0.0	Cardiogenic shock following myocardial infarction
6	52	23	40	0.9	30	13	2.2	4.5	CABG, aortic valve replacement, COPD
7	53	34	26	3.7	65	17	2.2	2.9	Aortic valve and arch replacement (type A dissection)
8	73	34	37	3.8	36	16	2.8	0.0	Aortic and mitral valve replacement, COPD
9	64	30	57	6.9	30	11	3.0	3.9	CABG, aortic valve replacement, mitral ring
10	69	24	44	19.8	25	26	3.1	0.0	Cardiogenic shock following myocardial infarction

BMI, body mass index; CABG, coronary artery bypass graft; COPD, chronic obstructive pulmonary disease; LOS, length of stay; LVEF, left ventricular ejection fraction; PAOP, pulmonary artery occlusion pressure; PBW, predicted body weight; SAPS, Simplified Acute Physiology Score.

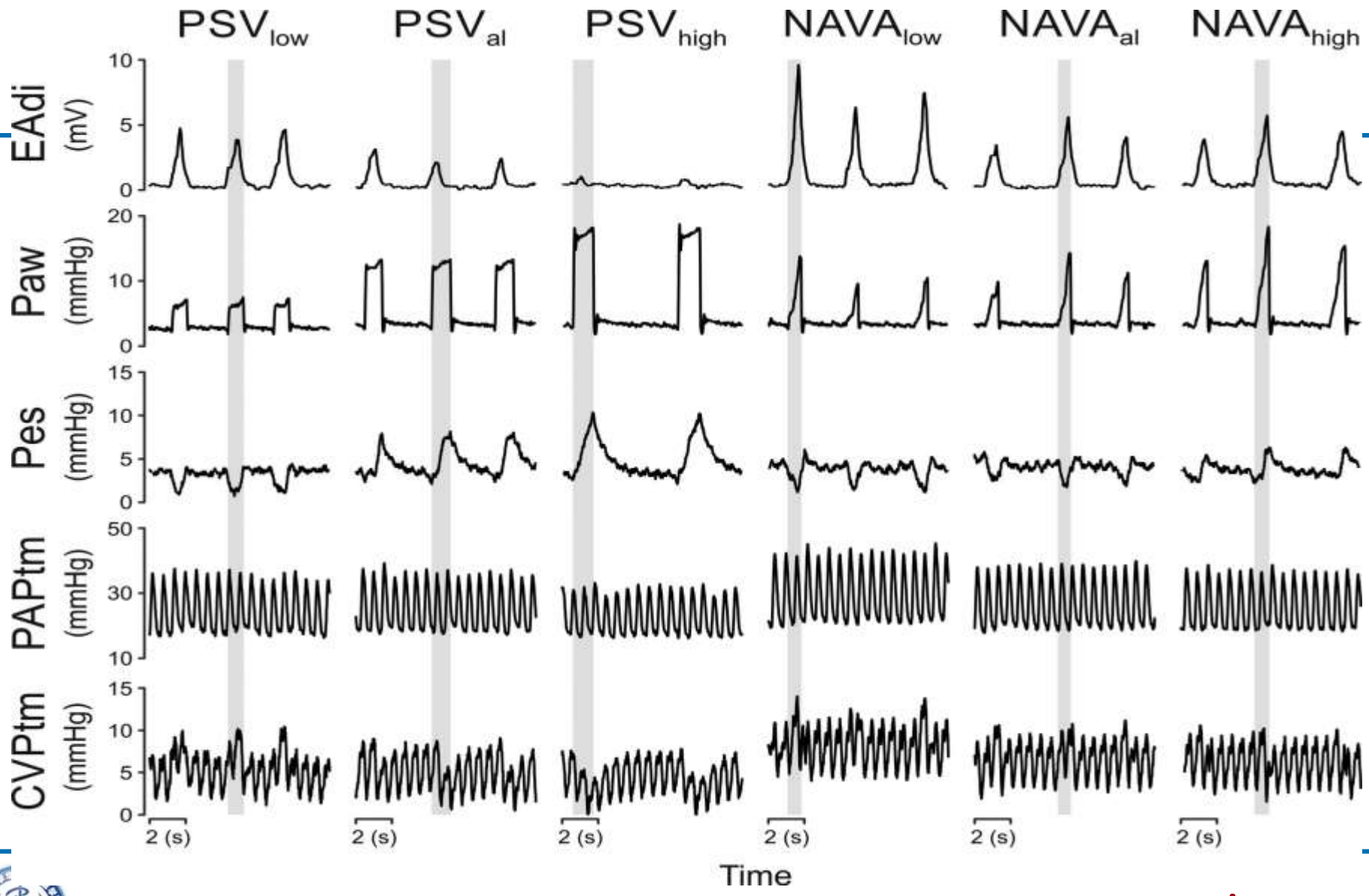
PSVlow
PSVal
PSVhigh
NAVAlow
NAVAal
NAVAhigh
EAdi (mV)
Paw (mmHg)
Pes (mmHg)
PAPtm (mmHg)
CVPtm (mmHg)
2 (s)
Time

Table 2 Blood gases, respiratory pattern and systemic hemodynamic data

	PSVlow	PSVal	PSVhigh	NAVAlow	NAVAal	NAVAhigh	*P* value		
							Level	Mode	Interaction
Blood gases									
PaO_2 (mmHg)	94 ± 21	94 ± 21	97 ± 21	94 ± 25	91 ± 25	94 ± 24	0.325	0.495	0.864
$PaCO_2$ (mmHg)	38 ± 9	37 ± 8	36 ± 8	39 ± 10	39 ± 11	38 ± 9	<0.001	0.202	0.102
SaO_2 (%)	97 ± 2	97 ± 1	98 ± 2	97 ± 2	97 ± 2	97 ± 2	0.174	0.309	0.782
pH	7.41 ± 0.1	7.43 ± 0.1	7.45 ± 0.1	7.42 ± 0.1	7.43 ± 0.1	7.43 ± 0.1	<0.001	0.464	0.164
Base excess	0.2 ± 3.6	0.3 ± 3.6	0.1 ± 3.6	0.4 ± 3.5	0.5 ± 3.5	0.5 ± 3.5	0.194	0.244	0.592
Respiratory pattern									
Respiratory rate (breaths/minute)	21 ± 5	18 ± 4	13 ± 3	20 ± 5	21 ± 5	20 ± 6	<0.001	0.041	<0.001
Tidal volume (ml/kg PBW)	6.3 ± 1.1	8.2 ± 1.8	11.4 ± 3.0	6.7 ± 1.2	7.0 ± 1.2	7.6 ± 1.2	<0.001	0.018	0.001
Minute ventilation (l/minute)	7.7 ± 2.0	8.6 ± 2.5	8.7 ± 2.1	8.1 ± 2.7	8.6 ± 2.5	8.7 ± 3.0	<0.001	0.619	0.361
Electrical activity of the diaphragm (% EAdi max)	61 ± 16	32 ± 11	17 ± 9	90 ± 33	71 ± 19	29 ± 25	<0.001	0.002	0.3
Mean inspiratory transpulmonary pressure (cmH_2O)	3 ± 4	5 ± 4	10 ± 4	3 ± 3	3 ± 4	7 ± 5	<0.001	0.158	<0.001
Mean esophageal pressure deflection (cmH_2O)	−0.7 ± 1.5	2.1 ± 1.9	4 ± 2.3	−1.5 ± 2.4	−1.5 ± 1.7	0 ± 1	0.001	<0.001	<0.001
Systemic hemodynamic data									
Pulmonary artery occlusion pressure (mmHg)	16 ± 7	14 ± 4	15 ± 7	15 ± 7	15 ± 5	16 ± 6	0.516	0.424	0.241
Mean systemic arterial pressure (mmHg)	65 ± 8	61 ± 9	65 ± 9	65 ± 9	63 ± 9	63 ± 9	0.065	0.922	0.256
Heart rate (beats/minute)	90 ± 9	90 ± 9	89 ± 9	89 ± 10	90 ± 10	88 ± 10	0.3	0.831	0.567
Cardiac output (l/minute)	4.7 ± 0.9	4.8 ± 0.7	4.8 ± 0.7	5.2 ± 1.2	5.1 ± 1.1	5.1 ± 1.2	0.964	0.082	0.284
Mixed venous oxygen saturation (%)	66 ± 7	64 ± 5	66 ± 9	63 ± 5	65 ± 7	62 ± 5	0.469	0.059	0.211

Table 3 Mean central venous and mean pulmonary artery pressures for the entire experimental period

	PSVlow	PSVal	PSVhigh	NAVAlow	NAVAal	NAVAhigh	*P* value		
							Level	Mode	Interaction
Expiratory values									
Central venous pressure (mmHg)	10 ± 3	10 ± 3	10 ± 3	11 ± 3	10 ± 3	11 ± 3	0.064	0.091	0.919
Mean pulmonary artery pressure (mmHg)	30 ± 8	27 ± 6	27 ± 6	30 ± 5	29 ± 5	28 ± 5	0.002	0.065	0.208
Transmural central venous pressure (mmHg)	3 ± 4	1 ± 5	2 ± 4	5 ± 4	2 ± 3	3 ± 3	0.06	0.267	0.566
Transmural mean pulmonary artery pressure (mmHg)	22 ± 9	18 ± 8	19 ± 7	24 ± 6	21 ± 5	21 ± 6	<0.001	0.091	0.683
Cyclic pressure changes									
Central venous pressure (mmHg)	−0.5 ± 0.4	0.4 ± 0.4	1.0 ± 0.4	−1 ± 0.5	−0.8 ± 0.6	−0.5 ± 0.7	<0.001	<0.001	<0.001
Mean pulmonary artery pressure (mmHg)	−2.2 ± 1.1	0.5 ± 1.4	2.5 ± 1.3	−3.2 ± 0.9	−2.7 ± 1.2	−1.9 ± 1	<0.001	<0.001	<0.001
Transmural central venous pressure (mmHg)	1.3 ± 1.6	0 ± 0.9	−0.9 ± 1.1	1.4 ± 2.4	1.6 ± 1.6	0.1 ± 1.8	0.009	0.08	0.03
Transmural mean pulmonary artery pressure (mmHg)	−0.3 ± 1.8	0.1 ± 0.8	0.5 ± 0.8	−0.8 ± 2.1	−0.4 ± 1.3	−1.2 ± 1.9	0.479	0.078	0.026

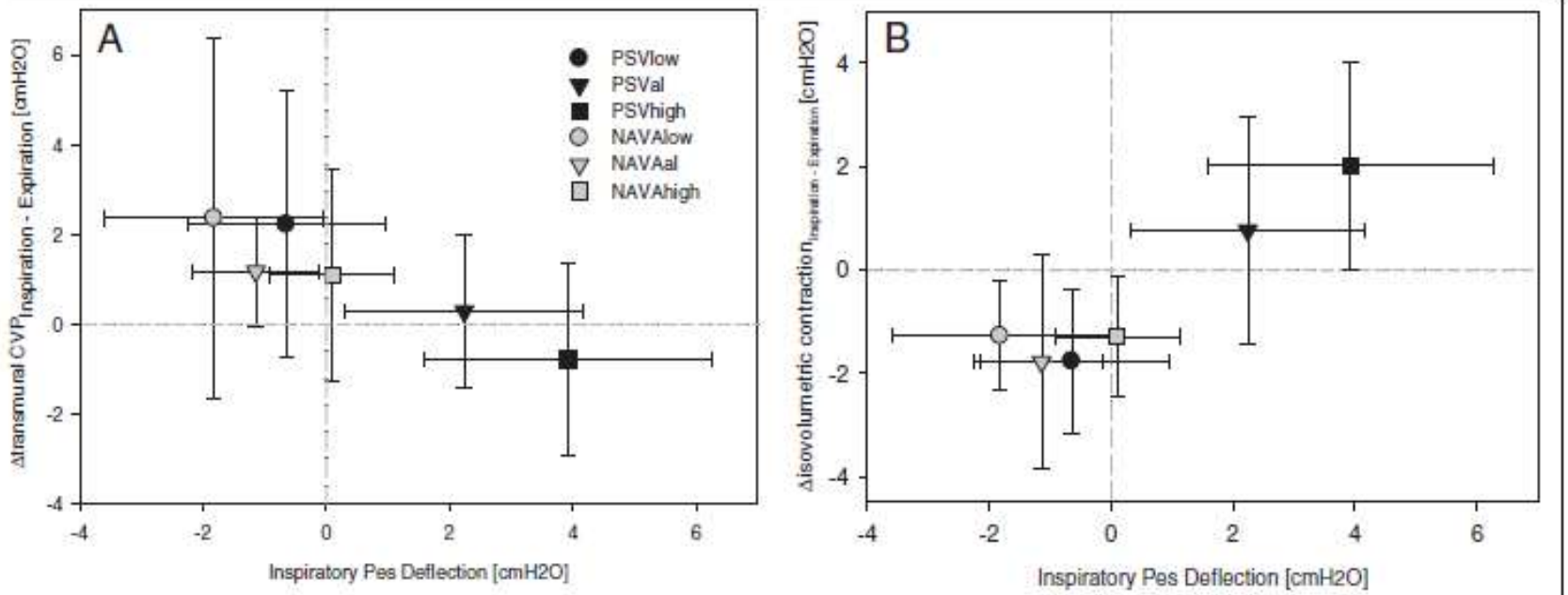

Figure 3 Loading conditions of the right ventricle in the average breath. Analysis of the single representative breath cycle. Central venous pressure was measured at the base of the c wave. **(A)** Inspiratory minus expiratory transmural central venous pressure (ΔCVP), $P = 0.015$ for level and mode. **(B)** Inspiratory minus expiratory transmural isvolumetric pressure (Δisovolumetric pressure), $P = 0.003$ for support level–ventilation mode interaction. Values presented as mean ± standard deviation. NAVA, neurally adjusted ventilator assist; NAVAal, adequate NAVA level identified by a titration procedure; NAVAhigh, 200% of the adequate NAVA level; NAVAlow, 50% of the adequate NAVA level; Pes, esophageal pressure; PSV, pressure support ventilation; PSVal, adequate level of pressure support ventilation identified on clinical grounds; PSVhigh, 150% of adequate PSV level; PSVlow, 50% of adequate PSV level.

Table 4 Loading conditions of the right ventricle in the average breath

	PSVlow	PSVal	PSVhigh	NAVAlow	NAVAal	NAVAhigh	*P* value		
							Level	Mode	Interaction
Transmural central venous pressures at c wave									
End expiratory (mmHg)	2.6 ± 4	1.3 ± 5.1	2.3 ± 4.1	4.2 ± 4.5	2.4 ± 2.5	3.1 ± 3.4	0.331	0.018	0.817
End inspiratory (mmHg)	4.8 ± 4.5	1.5 ± 4.3	1.5 ± 3.9	6.6 ± 3.0	3.6 ± 3.3	4.2 ± 2.2	0.001	0.1	0.697
Cyclic change (mmHg)	2.2 ± 3	0.3 ± 1.7	−0.8 ± 2.1	2.4 ± 4	1.2 ± 1.2	1.1 ± 2.4	0.015	0.015	0.303
Isovolumetric pressure generation									
Inspiratory transmural isovolumetric pressure (mmHg)	11 ± 4.6	12.3 ± 4.4	14 ± 4.6	11.5 ± 4.7	11.1 ± 4.6	10.8 ± 4.2	0.057	0.095	0.005
Expiratory transmural isovolumetric pressure (mmHg)	12.7 ± 4.7	11.5 ± 4.5	12 ± 5.2	12.8 ± 4.1	12.8 ± 3.7	12.1 ± 4.7	0.266	0.257	0.318
Cyclic change in transmural isovolumetric pressure (mmHg)	−1.8 ± 1.4	0.8 ± 2.2	2 ± 2	−1.3 ± 1	−1.8 ± 2.1	−1.3 ± 1.1	0.003	0.009	0.003
Total pressure generation									
Inspiratory transmural pressure generation (mmHg)	29.7 ± 10.7	27.2 ± 7.8	29.6 ± 9.4	29.8 ± 9.6	26.9 ± 8.5	26.9 ± 7	0.06	0.38	0.561
Expiratory transmural pressure generation (mmHg)	30.4 ± 10.8	23.5 ± 8.3	26.5 ± 9.4	28.6 ± 10.4	27.9 ± 8	27 ± 6.9	0.231	0.053	0.241
Cyclic change in transmural pressure generation (mmHg)	−0.7 ± 2.3	3.8 ± 8	3.1 ± 1.5	1.2 ± 3.7	−1 ± 4.5	0 ± 2	0.543	0.076	0.033

Table 5 Right ventricular echocardiographic data

Doppler flow profile in the right ventricular outflow tract ($n = 8$)	PSVlow	PSVal	PSVhigh	NAVAlow	NAVAal	NAVAhigh	*P* value		
							Level	Mode	Interaction
End expiration									
Acceleration time (milliseconds)	82 ± 14	83 ± 13	80 ± 11	82 ± 16	77 ± 14	89 ± 18	0.484	0.68	0.141
Flow period (milliseconds)	242 ± 25	256 ± 36	256 ± 37	240 ± 23	242 ± 27	243 ± 28	0.072	0.127	0.285
Maximum flow velocity (m/second)	0.8 ± 0.2	0.9 ± 0.3	0.8 ± 0.3	0.7 ± 0.3	0.8 ± 0.2	0.9 ± 0.3	0.047	0.012	0.465
Velocity time integral (cm)	13 ± 2	14 ± 3	14 ± 3	13 ± 2	13 ± 3	14 ± 3	0.009	0.063	0.178
End inspiration									
Acceleration time (milliseconds)	86 ± 15	81 ± 15	84 ± 17	81 ± 12	88 ± 20	91 ± 17	0.62	0.259	0.296
Flow period (milliseconds)	250 ± 27	242 ± 25	231 ± 33	250 ± 21	261 ± 29	251 ± 30	0.02	0.067	0.028
Maximum flow velocity (m/second)	0.8 ± 0.2	0.8 ± 0.3	0.7 ± 0.2	0.7 ± 0.3	0.9 ± 0.3	0.8 ± 0.3	0.168	0.154	0.166
Velocity time integral (cm)	13 ± 3	13 ± 3	12 ± 3	13 ± 2	14 ± 3	14 ± 3	0.154	0.046	0.025
Inspiratory values as percentage of expiratory values									
cAcceleration time (%)	104 ± 8	98 ± 8	105 ± 10	101 ± 13	115 ± 9	104 ± 11	0.617	0.217	0.012
Flow period (%)	103 ± 2	94 ± 3	91 ± 2	104 ± 2	107 ± 3	103 ± 2	<0.001	<0.001	<0.001
Maximum flow velocity (%)	99 ± 2	92 ± 7	86 ± 8	100 ± 3	106 ± 5	97 ± 4	<0.001	0.003	<0.001
Velocity time integral (%)	101 ± 3	89 ± 6	83 ± 9	103 ± 4	109 ± 5	100 ± 4	<0.001	<0.001	<0.001

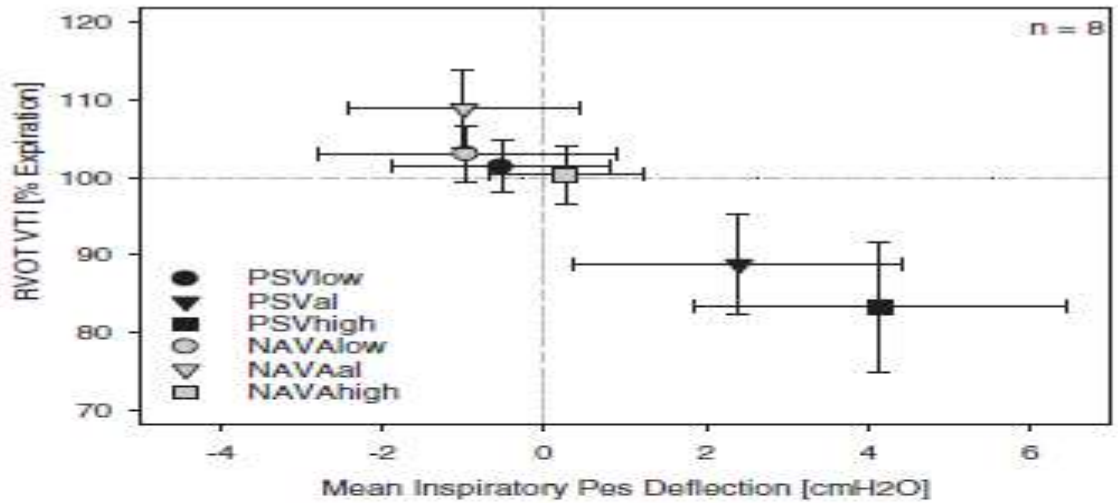

Figure 4 Right ventricular outflow during the respiratory cycle. The velocity time integral in the inspiratory right ventricular outflow tract (RVOT VTI) as a percentage of its expiratory value. There is a significant increase in RVOT VTI during inspiration for all NAVA levels compared to PSV ($P < 0.001$, level*mode interaction). Data presented as mean ± standard deviation. NAVA, neurally adjusted ventilator assist; NAVAal, adequate NAVA level identified by a titration procedure; NAVAhigh, 200% of the adequate NAVA level; NAVAlow, 50% of the adequate NAVA level; Pes, esophageal pressure; PSV, pressure support ventilation; PSVal, adequate level of pressure support ventilation identified on clinical grounds; PSVhigh, 150% of adequate PSV level; PSVlow, 50% of adequate PSV level.

Discussion

- The main finding of this study was that ventilation with NAVA in patients with impaired cardiac function but stable hemodynamics avoided an inspiratory increase in right ventricular outflow impedance by preserving the cyclic, negative deflections in intrathoracic pressure via feedback control of transpulmonary pressure and tidal volume.

- In contrast, increased inspiratory assist with PSV progressively increased right ventricular outflow impedance, transpulmonary pressure, and tidal volume.

- The pattern of decreasing right and increasing left ventricular stroke volume during inspiration is the characteristic pattern of heart–lung interactions during positive pressure ventilation

- The transmural pressure at the base of the c wave of the CVP tracing, a surrogate of right ventricular end-diastolic wall tension, decreased slightly but significantly with increasing support both in inspiration and expiration without difference between modes. This result should be interpreted with caution, since pleural pressure may not adequately reflect pericardial pressure。

- Nevertheless, even if changes in preload were involved, the increased right ventricular isovolumetric contraction pressure in the presence of reduced RVOT VTI indicates increased impedance to right ventricular ejection in inspiration with PSV, and the opposite changes indicate reduced impedance to ejection during inspiration with NAVA

Study limitations

- Several limitations must be addressed. The study was carried out to demonstrate the underlying physiology; due to safety concerns, patients with impaired cardiac function but stable hemodynamic and metabolic conditions were studied for short periods only.
- Most of the patients were studied during the first day after cardiac surgery. Despite being clinically stable, some of these patients could have had relevant intravascular volume changes.
- There is no standard approach to titrate NAVA.
- The resulting relatively high PSV can be criticized for augmenting the effects of PSV on right ventricular function. However, most patients were likely to have reduced chest wall compliance due to obesity and recent cardiac surgery.
- PEEP may influence respiratory drive and assist requirements , but PEEP was kept constant and should not have influenced the changes within patients.

Conclusions

- In patients with impaired cardiac function, right ventricular performance is less impaired during NAVA titrated to the breathing pattern compared with PSV selected based on clinical criteria. Proposed mechanisms are preservation of cyclic intrathoracic pressure changes characteristic of spontaneous breathing and limitation of right-ventricular outflow impedance during inspiration, regardless of the NAVA level.
- Thus, NAVA not only prevents lung overdistension and potentially diaphragm disuse, but also the characteristic side effects of positive pressure ventilation on right ventricular function.


谢谢聆听
欢迎提问
2002 3 30